

Sharpless 四唑合成中捕获双四唑锌配合物

王立中¹ 王锡森¹ 李咏华¹ 白志平^{*·1} 熊仁根^{*·1} 熊 明² 李国武²

(¹南京大学配位化学研究所, 配位化学国家重点实验室, 南京 210093)

(²中国地质大学地球科学实验室, 北京 100083)

关键词: 双四唑 水热合成 锌配位聚合物

分类号: O614. 24^{*·1}

Trapping of Zn-Complex with Bis(tetrazole) Ligand during the Demko-Sharpless' Tetrazole Synthesis

WANG Li-Zhong¹ WANG Xi-Sen¹ LI Yong-Hua¹ BAI Zhi-Ping^{*·1}

XIONG Ren-Gen^{*·1} XIONG Ming² LI Guo-Wu²

(¹ Coordination Chemistry Institute, The State Key Laboratory of Coordination Chemistry, Nanjing University, Nanjing 210093)

(² Geoscience Laboratories, China University of Geosciences, Beijing 100083)

The reaction of malononitrile with $ZnCl_2$ and NaN_3 in the presence of 2, 2'-bipyridine and water affords the first bis(tetrazole) Zn-complex intermediate, mono(2, 2'-bipyridine) bis(tetrazolyl) methane aqua zinc (II), $[Zn(2, 2'-bpy)(BTZ)(H_2O)] \cdot (H_2O)_2$ (**1**) which gives a clue for Demko-Sharpless' tetrazole synthesis. Crystal data for **1**: $C_{13}H_{18}N_{10}O_4Zn$, $M_r = 443.74$, monoclinic, space group $P2_1/c$, $a = 12.5705(18)$, $b = 16.078(2)$, $c = 9.1921(13)\text{\AA}$, $\beta = 95.010(3)^\circ$, $V = 1850.7(5)\text{\AA}^3$, $Z = 4$. CCDC: 197788.

Keywords: bis-tetrazole hydrothermal synthesis zinc coordination polymer

Tetrazoles ligands have found a wide applications in coordination chemistry, medicinal chemistry and material science^[1]. It is very important for us to further explore their novel and environment-friendly synthesis method. Recently, Demko and Sharpless have successfully reported a safe, convenient and environmentally friendly procedure for the synthesis of 5-substituted 1H-tetrazoles in water^[2]; this efficient, new synthetic approach offers exciting and fascinating prospects for the simple generation of a variety of new

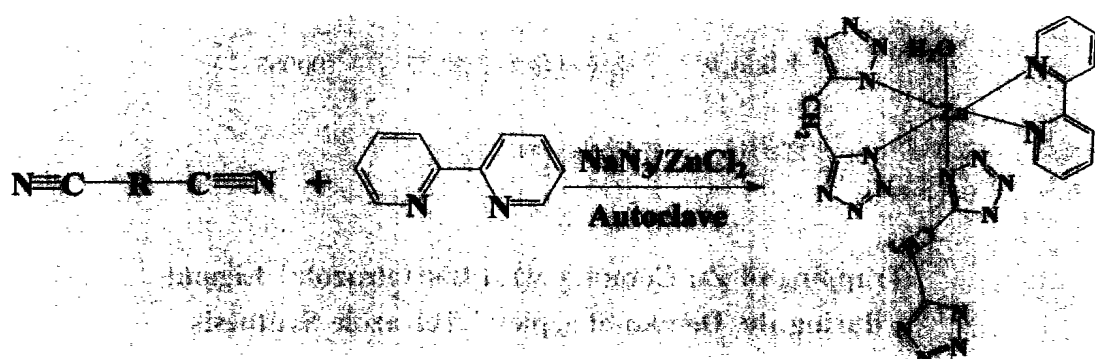
compounds. Generally, 1H-tetrazole or bi-1H-tetrazole derivatives are prepared by the addition of azide to nitriles in water using zinc salts as catalysts (Scheme 1). The role of the zinc in this reaction is unclear but it is suggested that the solid intermediate from the reaction of PhCN with $ZnBr_2$ and NaN_3 is $(PhCN_3)_2Zn$ even though we have successfully trapped some intermediates during Demko-Sharpless' tetrazole synthesis. The structural characterization of such an intermediate may provide important clues to the mechanistic role of zinc

收稿日期: 2002-09-08。收修改稿日期: 2002-10-28。

国家重点基础研究发展计划资助项目(G2000077500)、国家自然科学基金资助项目和教育部优秀青年教师资助计划项目。

* 通讯联系人。E-mail: baizp@ netra. nju. edu. cn; xiongrg@ netra. nju. edu. cn

第一作者: 王立中, 男, 29岁, 硕士生, 研究方向: 功能材料及其合成。



in this reaction that in turn may allow synthetic chemists to further optimize this reaction. To date, it still remains a great challenge for us to trap the intermediates with multi-tetrazole during this reaction system.

In our continuous research we have combined metal salts with potentially bridging organic ligands under hydrothermal conditions^[3] to produce a range of new materials. Our experience with such systems prompted an investigation of the nature of the solid intermediate in the Demko-Sharpless reaction. Specifically we have undertaken structural study of the product or “intermediate” formed by the hydrothermal reaction of $ZnCl_2$ with malononitrile and NaN_3 in water in the presence of 2, 2'-bipyridine (Scheme 2). As expected, the reaction affords $[Zn(2, 2'-bpy)(BTZ)(H_2O)] \cdot (H_2O)_2$ (**1**), with 1, 2-bis(tetrazolyl) methane (BTZ) ligand. Herein we report the synthesis, characterization and solid state structure of the intermediate^[4].

In the presence of 2, 2'-bipy the reaction of $ZnCl_2$ with NaN_3 and malononitrile in water at 160°C yields the products **1**. The IR spectrum indicated the absence of the cyano group which is consistent with the 2 + 3 cycloaddition between the cyano group and the azide^[2]. Moreover, a strong and broad peak at its IR spectrum (3200cm^{-1} , as shown in Fig. 1) suggests there may be

water molecules in **1** which is confirmed by crystal structure determination later.

Compound **1** has a formula of $Zn(2, 2'-bpy)(BTZ)(H_2O)] \cdot (H_2O)_2$ in which the BTZ acts as a tridentate ligand and links two zinc atoms through the three nitrogen atoms of the bis-tetrazole rings in which one comes from tetrazole ring and other two belong to other tetrazole ring^[5]. The local coordination geometry around each zinc atom can be best described as a slightly distorted octahedron formed by five nitrogen atoms of one 2, 2'-bpy, two BTZ ligands and one oxygen atom of water, as shown in Fig. 2. Thus each BTZ ligand bridges two zinc atoms to result in the formation of 1D infinite chain (Fig. 3a and 3b). Also it is interesting to note that strong hydrogen-bonds have been

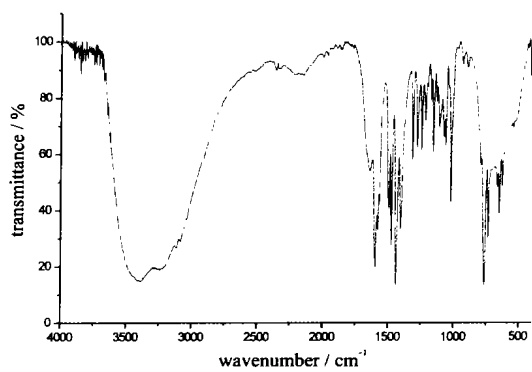


Fig. 1 IR spectrum of coordination polymer **1**

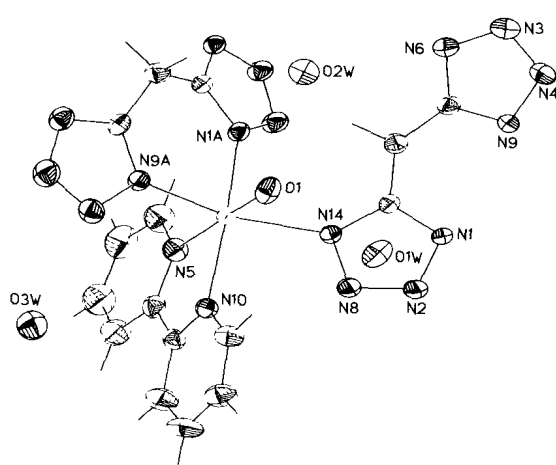


Fig. 2 Asymmetric unit representation of coordination polymer **1** in which typical bond lengths are as follows:
 $\text{Zn}(1)\text{-N}(1)$ 2.107(3); $\text{Zn}(1)\text{-N}(5)$ 2.182(3);
 $\text{Zn}(1)\text{-N}(9\text{A})$ 2.105(3); $\text{Zn}(1)\text{-N}(14)$ 2.097;
 $\text{Zn}(1)\text{-O}(1)$ 2.441(3) \AA

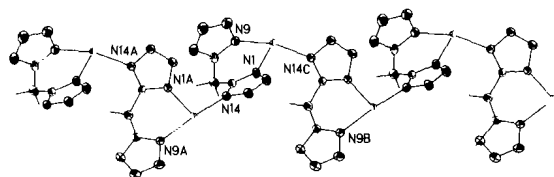


Fig. 3a 1D infinite chain representation of coordination polymer **1** in which 2,2'-bipyridine and uncoordinated water molecules are omitted for clarity



Fig. 3b 1D infinite chain representation of coordination polymer **1** in which Zn octahedron is highlighted

found among the nitrogen atoms of bis-tetrazole ligand and uncoordinated water molecules to result in the formation of three-dimensional network, as shown in Fig. 4.

Although compound **1** contains a 2,2'-bpy ligand, the successful generation of the BTZ ligand in compounds **1** strongly supports Demko-Sharpless new

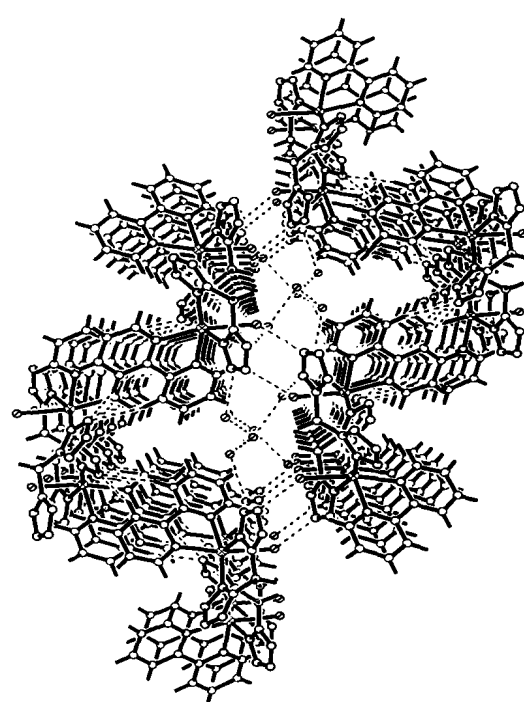


Fig. 4 Packing representation of coordination polymer **1** along with *c*-axis

synthesis method of bis-tetrazole. However, the situation is quite different from that found in the reaction system of ZnCl_2 and $\text{N}, \text{N}'\text{-dicyanohydrazine}$ in which an N-N bond cleavage has occurred in the Demko-Sharpless' tetrazole synthesis.

The solid state fluorescent spectrum (Fig. 5) of **1** at room temperature shows that maximal emission peak occurred in 410 nm, suggesting **1** may be good blue-light-emitted material. The photoluminescent mecha-

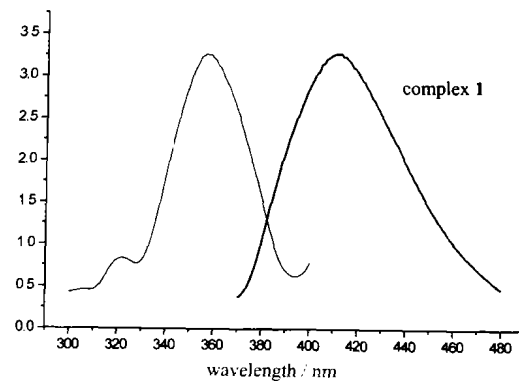


Fig. 5 Solid state fluorescent emission spectrum of coordination polymer **1** at room temperature (left = excitation. $\lambda_{\text{max}} = 352\text{nm}$; right = emission. $\lambda_{\text{max}} = 410\text{nm}$)

nism may be considered lignd-to lignd transition, which is in fairly good agreement with these Zn-coordination polymers^[6].

In conclusion, apart from affording a new insights into the nature of the solid formed in the Demko-Sharpless reaction, the work described provides strong encouragement that novel metal coordination polymer may be produced by the hydrothermal generation of bridging ligand in the presence of appropriate metal ions.

Supporting Information Available: An X-ray crystallographic file (CIF) is requested from Dr. Ren-Gen Xiong at XIONGRG@netra.nju.edu.cn.

References

- [1] (a) Carlucci L., Ciani G., Proserpio D. M. *Angew. Chem. Int. Ed.*, **1999**, *38*, 3488;
 (b) Singh H., Chawla A. S., Kapoor V. K., Paul D., Malhotra R. K. *Prog. Med. Chem.*, **1980**, *17*, 151;
 (c) Ostrovskii V. A., Pevzner M. S., Kofmna T. P., Sheherbinin M. B., Tselinskii I. V. *Targets Heterocycl. Syst.*, **1999**, *3*, 467;
 (d) Janiak C., Scharmann T. G., Gunter W., Girgsdies F., Hemling H., Hinrichs W., Lentz D. *Chem. Eur. J.*, **1995**, *1*, 637;
 (e) Bhandari S., Mahon M. F., Molloy K. C., Palmer J. S., Sayers S. F. *J. Chem. Soc. Dalton Trans.*, **2000**, 1053.
- [2] (a) Demko Z. P., Sharpless K. B. *J. Org. Chem.*, **2001**, *66*, 7945;
 (b) Demko Z. P., Sharpless K. B. *Org. Lett.*, **2001**, *3*, 4091.
 [3] (a) Xiong R.-G., You X.-Z., Abrahams B. F., Xue Z., Che C.-M. *Angew. Chem. Int. Ed.*, **2001**, *40*, 4422;
 (b) Xiong R.-G., Zhang J., Chen Z.-F., You X.-Z., Che C.-M., Fun H.-K. *J. Chem. Soc. Dalton Trans.*, **2001**, 780;
 (c) Xue X., Wang X.-S., Xiong R.-G., You X.-Z., Abrahams B. F., Che C.-M., Ju H.-X. *Angew. Chem. Int. Ed.*, **2002**, *41*, 2944;
 (d) Zeng X.-R., Xiong R.-G., You X.-Z., Raj S. S. S., Fun H.-K. *Chin. J. Inorg. Chem.*, **2000**, *16*, 641.
 [4] (a) Xiong R.-G., Xue X., Zhao H., You X.-Z., Abrahams B. F., Xue Z. *Angew. Chem. Int. Ed.*, **2001**, *41*, 3800;
 (b) Xue X., Abrahams B. F., Xiong R.-G., You X.-Z. *Aust. J. Chem.*, **2002**, *55*, 495;
 (c) Xue X., Wang X.-S., Wang L.-Z., Xiong R.-G., You X.-Z., Che C.-M., Xue Z. *Inorg. Chem.*, **2002**, in press.
 [5] Crystal Data for **1**: $C_{13}H_{18}N_{10}O_4Zn$, $M_r = 443.74$, monoclinic, $P2_1/c$, $a = 12.5705(18)$, $b = 16.078(2)$, $c = 9.1921(13)\text{\AA}$, $\beta = 95.010(3)^\circ$, $V = 1850.7(5)\text{\AA}^3$, $Z = 4$, $D_c = 1.593\text{Mg}\cdot\text{m}^{-3}$, $R_1 = 0.0501$, $wR_2 = 0.1442$, $T = 293\text{K}$, $\mu = 1.372\text{mm}^{-1}$, $S = 1.025$.
 [6] (a) Xiong R.-G., Zuo J.-L., You X.-Z., Abrahams B. F., Bai Z.-P., Che C.-M., Fun H.-K. *Chem. Commun.*, **2000**, 2061;
 (b) Xiong R.-G., Zuo J.-L., You X.-Z., Fun H.-K., Raj S. S. S. *Organometallics*, **2000**, *19*, 4183;
 (c) Fun H.-K., Raj S. S. S., Xiong R.-G., Zuo J.-L., Yu Z., You X.-Z. *J. Chem. Soc., Dalton Trans.*, **1999**, 1915;
 (d) Zhang J., Lin W. B., Chen Z.-F., Xiong R.-G., Abrahams B. F., Fun H.-K. *J. Chem. Soc., Dalton Trans.*, **2001**, 1804.

Ce-Zr-Ba-O 纳米材料的制备及其结构与性能研究

张培壮¹ 陈 敏^{*,1} 王月娟² 郑小明¹

(¹ 浙江大学催化研究所, 杭州 310028)

(² 浙江师范大学物理化学研究所, 金华 321004)

以金属硝酸盐为原料, 分别采用高分子前驱体法、柠檬酸盐凝胶法制备了纳米级的 Ce-Zr-Ba-O 复合氧化物超细粒子, 采用 X- 射线衍射(XRD)、透射电镜(TEM)、BET 比表面测定、热重 - 差热(TG-DTA)技术对催化剂进行了表征, 并考察了催化剂的 CO 氧化活性和热稳定性。实验结果表明, 高分子前驱体法和柠檬酸盐凝胶法制备的催化剂粉体都达到了纳米级。两种方法中, 高分子前驱体法所制得的催化剂的 BET 比表面达 $118.96 \text{ m}^2 \cdot \text{g}^{-1}$, CO 氧化反应活性较高, 同时该方法制得的催化剂分散性好、无团聚, 经 1000°C 高温焙烧后仍基本无烧结、无团聚现象, 具有较高的热稳定性。

关键词:	制备方法	纳米粒子	Ce-Zr-Ba-O	催化剂
分类号:	0611. 4	0614. 33 ^{1,2}	0614. 41 ^{1,2}	

Ce-Zr 复合氧化物以其独特的催化性能和储放氧功能^[1, 2], 引起了广大科技工作者的关注, 然而不同的制备方法, 不同的助剂添加效应, 直接影响到催化剂的活性、比表面、热稳定性等。已有大量文献报导了 Ce-Zr 复合氧化物的优良性能。中国科技大学的肖莉等^[3]研究了 Ce-Zr 固溶体在三效催化剂中的作用, 表明其具有较好的储氧性能并能降低三效催化剂的起燃温度。Christine Bozo 等^[4]研究了 CH_4 在 $\text{Pt}/\text{CeO}_2-\text{ZrO}_2$ 催化剂上的燃烧反应, 其催化活性远比 $\text{Pt}/\text{Al}_2\text{O}_3$ 高得多。F. Zamar 等^[5]也研究了在 CeO_2 中添加 Zr 制备 CH_4 燃烧催化剂, 增强了 CeO_2 催化剂的 Redox 性能, 提高了催化剂的低温活性。

由于 TWC 三效催化剂的工作环境在较高温度下使用, 因而其活性会发生变化, 因此研制和开发稳定性较好的载体已成为研究热点之一。郭耘等^[6]在 $\text{Pt}/\text{Al}_2\text{O}_3$ 体系中添加了 BaO , 制成 $\text{Pt}/\text{BaO}-\text{Al}_2\text{O}_3$ 体系催化剂, 发现 BaO 的引入在一定程度上增强了 $\text{Pt}/\text{Al}_2\text{O}_3$ 的 CO 氧化的热稳定性, 同时提高了 $\text{Pt}/\text{Al}_2\text{O}_3$ 的 CO 氧化活性, 降低了 CO 的完全转化温度。

由于目前采用常规的一些制备方法制出的 Ce-Zr 复合氧化物粉体材料存在粒径大, 易团聚, 比

表面积小, 高温易烧结等问题。随着纳米材料研究的深入, 把纳米技术引入 Ce-Zr 复合氧化物的制备工作中是一个十分有意义的研究课题。Jones 等^[7]曾采用非水溶剂如苯, 醇等有机溶剂洗涤的方法, 但该方法存在消耗大量有机溶剂的弊端。酒金婷等^[8]采用高分子表面修饰共沸蒸馏工艺合成了无团聚的纳米氧化锆, 并运用于润滑脂中, 改善了其耐磨性能。本文通过高分子前驱体法和柠檬酸盐凝胶法制备出了纳米级的 Ce-Zr-Ba-O 复合氧化物, 并进行了比较, 发现采用高分子前驱体法可获得粒径均匀, 基本无团聚的纳米 Ce-Zr-Ba-O 复合氧化物, 该材料具有高比表面, 高热稳定性及较好的 CO 氧化能力, 这一研究结果为该材料在汽车尾气催化剂(TWC)中的应用提供了有意义的信息。

1 实验部分

1.1 催化剂的制备

1.1.1 高分子前驱体法

在聚乙二醇(分子量 20000)水溶液中缓慢滴加一定浓度的 $\text{Ce}(\text{NO}_3)_3 \cdot 6\text{H}_2\text{O}$ 、 $\text{Zr}(\text{NO}_3)_4 \cdot 5\text{H}_2\text{O}$ 、 $\text{Ba}(\text{NO}_3)_2$ 的混合溶液(摩尔比 $\text{Ce}: \text{Zr}: \text{Ba} = 7: 3: 1$)和氨水溶液并搅拌, 调节溶液 $\text{pH} > 9$ 后, 将溶液放入

收稿日期: 2002-07-03。收修改稿日期: 2002-09-25。

* 通讯联系人。E-mail: zhangpei@163.net

第一作者: 张培壮, 男, 25 岁, 硕士研究生; 研究方向: 多相催化。

冰箱中老化 24h, 抽滤, 将其溶于过量正丁醇中, 进行共沸蒸馏, 然后在 600℃ 烧烧 4h。制得 Ce-Zr-Ba-O 复合氧化物。

1.1.2 柠檬酸盐凝胶法

按化学计量比称取 $\text{Ce}(\text{NO}_3)_3 \cdot 6\text{H}_2\text{O}$ 、 $\text{Zr}(\text{NO}_3)_4 \cdot 5\text{H}_2\text{O}$ 、 $\text{Ba}(\text{NO}_3)_2$ 溶解于蒸馏水中, 加入一定量的络合剂和柠檬酸, 用氨水调节溶液呈微酸性, 蒸干溶液得无色透明凝胶, 将此凝胶于 120℃ 条件下烘干 24h, 最后于马弗炉中 600℃ 空气气氛下烧烧 4h。

1.2 催化剂结构测定和表征

1.2.1 X-射线衍射分析

XRD 分析实验在 Rigaku D/max-3 B X 衍射仪上进行, XRD 测得的粒径采用 Scherrer 公式计算。

1.2.2 TEM 分析

催化剂的形貌和粒子大小在 JEM-200CX 型透射电镜上进行观察并拍照, 仪器工作电压为 160kV, 相机长度为 55cm。

1.2.3 BET 比表面测定

样品的 BET 比表面测定在 OMNISORP. 100CS 型比表面测定仪上进行, 采用液氮温度下 N_2 吸附的方法。

1.2.4 TG-DTA 分析

凝胶试样的热重 - 差热分析在美国 PE 公司的 TGA-7 型热天平和 DTA-7 型高温差热仪上 N_2 气氛下进行, 温度范围 40 ~ 800℃。

1.3 反应性能测定

1.3.1 CO 氧化活性评价

采用微反装置评价催化剂的 CO 完全氧化活性, 催化剂装量 120mg, 反应气流量 $30\text{mL} \cdot \text{min}^{-1}$, 采用 SP-2304 气相色谱仪分析, 热导检测器检测。

2 结果与讨论

2.1 催化剂结构、粒度测定

图 1 是两种不同方法制备的催化剂的 XRD 图谱。由图可见, 两种不同方法制备的催化剂上均出现了 $\text{Ce}_{0.75}\text{Zr}_{0.25}\text{O}_2$ 的特征峰 (d 值为 3.09、1.89、1.61) 和 BaO 的特征峰 (d 值为 3.09、2.67、1.89), 由 XRD 结果来看 BaO 与 Ce-Zr 固溶体形成了同晶型, 空间群均为 $Fm\bar{3}m$ (225)。通过 XRD 指标化计算得知二相晶胞参数十分接近, 分别为: Ce-Zr 固溶体 $a = 5.349\text{\AA}$; BaO 的 $a = 5.335\text{\AA}$, 二晶系均为立方晶系, 虽然在 XRD 图中未能发现单独的 BaO 峰, 但由

于 BaO 的掺杂, 在结构上对阻碍 Ce-Zr 固溶体晶化, 粒子变细, 比表面增大起了十分重要的作用, 从而有利于该材料性能的提高。另外由 XRD 图来看, B 样品的谱峰比 A 样品宽化明显, 所以高分子前驱体法制备的粉体具有比柠檬酸盐法更小的一次粒子尺寸, 这表明不同的制备方法对催化剂微粒大小形成情况有明显影响, 这一点也由下面的 TEM 实验得到证实。

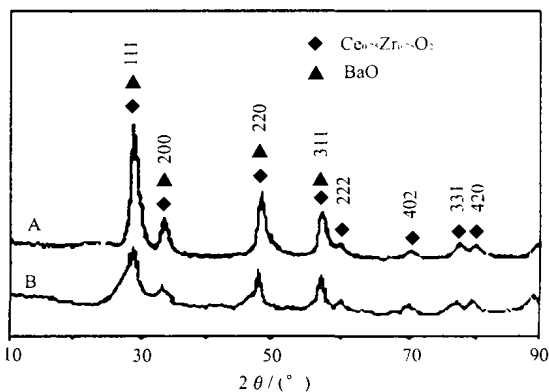


图 1 两种方法制备的催化剂粉体的 XRD 谱图

Fig. 1 XRD pattern of the Ce-Zr-Ba-O samples prepared by (A) citrate gel and (B) polymeric precursor methods

图 2 和图 3 是采用两种不同制备方法制得的催化剂的 TEM 照片和选区电子衍射照片。由图 3 的选区电子衍射照片可见, 两种方法制得的催化剂晶粒的衍射光环明显宽化, 说明复合氧化物粉体粒子是由纳米尺寸的晶粒组成。由图 2 的 TEM 照片比较催化剂的微观形貌, 可以发现, 高分子前驱体法制备的样品呈超细微粒, 形状多为球形或近似于球形, 且分布好, 这可能与制备过程中加入表面活性剂以及采用正丁醇共沸蒸馏改善了 Ce-Zr-Ba-O 粒子的团聚状况有关, 对提高粒子分散性有利。相比较而言, 柠檬酸盐凝胶法制得的样品颗粒分散不均匀, 出现了团聚现象。

2.2 BET 比表面分析

表 1 列出了两种方法制备的催化剂的比表面测定结果以及 XRD 法和 TEM 法测得的粒径数据。TEM 测得的是二次粒子 (亚微观), 而 XRD 测得的是一次粒子 (微观), 虽然在粒径大小上有一定差别, 但由表 1 可以清楚地看出, TEM 的粒径结果与 XRD 采用半峰宽法计算的结果成顺变规律。相比较, 高分子前驱体法制得的样品获得了较高的比表面, 达 $118.96\text{m}^2 \cdot \text{g}^{-1}$, 比 Fornasiero^[9] 报导的高比表面

表 1 两种方法制备的催化剂的 BET 比表面和粒径对照表

Table 1 BET Surface Areas, Grain Size of Catalysts Prepared by Two Methods

sample	BET surface areas / ($\text{m}^2 \cdot \text{g}^{-1}$)	XRD grain size / nm	TEM grain size / nm
polymeric precursor method	118.96	6.3	45
citrate gel method	38.60	7.3	55

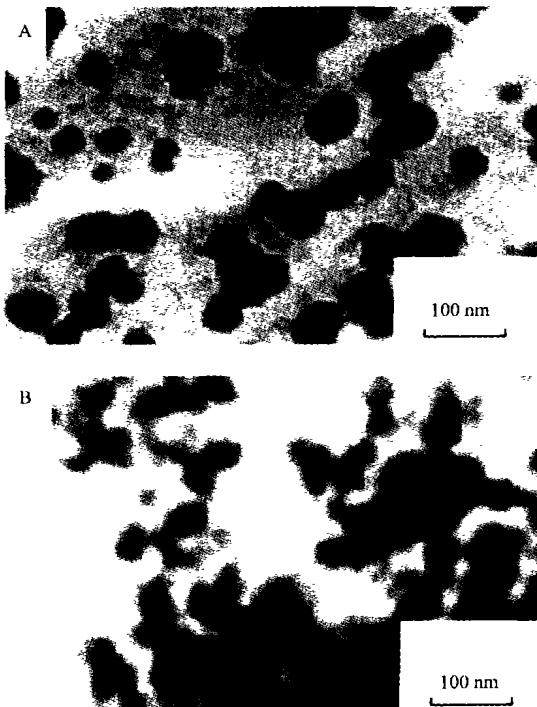


图 2 两种方法制备的催化剂粉体的 TEM 照片

Fig. 2 TEM micrographs of the Ce-Zr-Ba-O samples prepared by (A) polymeric precursor and (B) citrate gel methods

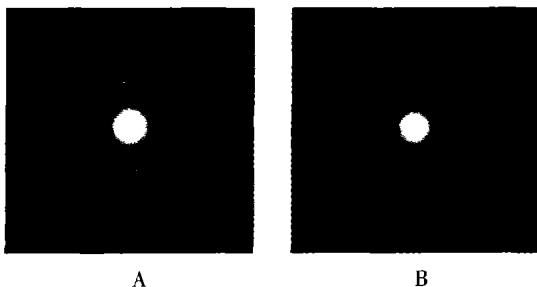


图 3 两种方法制备的催化剂粉体的晶相选区衍射图

Fig. 3 Diffraction patterns of the Ce-Zr-Ba-O samples prepared by (A) polymeric precursor and (B) citrate gel methods

Ce-Zr 复合氧化物结果约高 1 倍。高分子前驱体法制备的催化剂 BET 比表面较大, 分析其原因, 一是因为其粒度分布好, 基本没有出现团聚现象; 二是因为催化剂用正丁醇蒸馏过后, 脱除了孔道中的水, 在干燥焙烧过程中孔道不会因为水分的蒸发而崩塌, 从而维持了高比表面。另外, 柠檬酸盐凝胶法制备的

催化剂虽然达到纳米级, 但由于制备方法中不可避免的孔道中水分蒸发时的表面张力, 使得催化剂的孔道坍塌, 造成比表面下降。

2.3 热分析结果

图 5 是两种不同方法制得的样品 DTA 图谱。由图可见, 柠檬酸盐凝胶法制备的样品在 200°C 以前出现了吸热峰(图 5B), TG 曲线上也出现了相应的失重(图 4B), 这是样品中脱去吸附水的过程; 而高分子前驱体法制得的样品没有出现脱水吸热峰和失重台阶。这表明, 经正丁醇共沸蒸馏能非常有效的脱除催化剂中的残留水分。图 5 的 DTA 图谱中样品在 300°C 左右的放热峰对应于 TG 图谱上 250~400°C 的失重区, 这是由碳化的有机物(如柠檬酸)分解脱去以及凝胶脱去羟基而引起的。采用高分子前驱体法制得的样品 DTA 曲线上出现的 288°C 放热峰还包

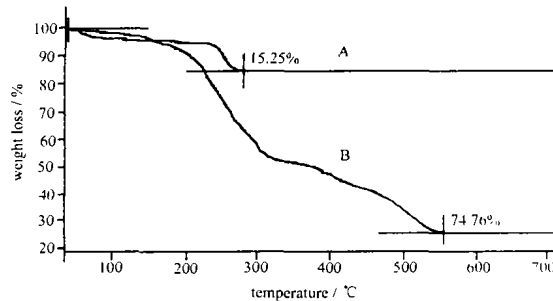


图 4 两种方法制备的催化剂干凝粉的热重(TG)图

Fig. 4 TG profiles of the Ce-Zr-Ba-O samples prepared by (A) polymeric precursor and (B) citrate gel methods

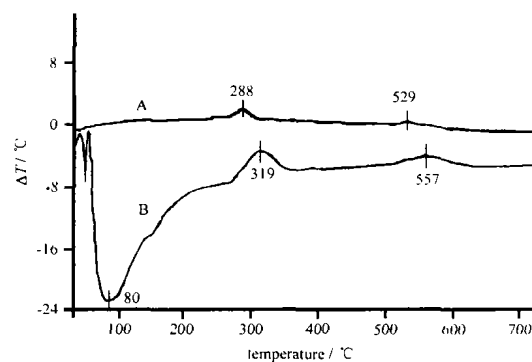


图 5 两种方法制备的催化剂干凝粉的差热(DTA)图

Fig. 5 DTA profiles of the Ce-Zr-Ba-O samples prepared by (A) polymeric precursor and (B) citrate gel methods

括了部分存在凝胶网络中的正丁醇等的脱除。两种方法制备的催化剂的 DTA 曲线在 520~560℃附近均出现了放热峰而并不伴随 TG 曲线的失重，结合 XRD 结果不难看出，这是由 Ce-Zr 固溶体晶相形成引起的。另外高分子前驱体法的晶相形成温度低与其形成的 Ce-Zr-Ba-O 颗粒基本无团聚有关，此结果与 XRD、TEM 相关联。

2.4 CO 氧化活性比较

图 6 是两种不同方法制备的催化剂的 CO 氧化活性评价结果。由图可见，两种方法制备的催化剂上催化活性有着较大的差别，高分子前驱体制得的样品 CO 完全转化温度为 280℃，明显优于柠檬酸盐凝胶法制得的催化剂，并且比文献报道的 Ce-Zr 复合氧化物低 200℃^[10]。究其原因，首先由于纳米微粒的表面效应和尺寸效应，使其反应活性大大增强，其次与制备过程中高分子表面修饰剂聚乙二醇（分子量 20000）的空间位阻抑制了前驱体颗粒长大有关。

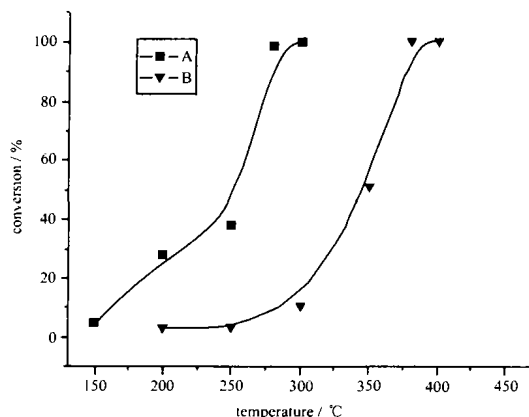


图 6 两种方法制备的催化剂的 CO 氧化活性比较

Fig. 6 CO oxidation activity of the Ce-Zr-Ba-O sample prepared by (A) polymeric precursor and (B) citrate gel methods

2.5 高温稳定性能考察

为了考察性能较好的高分子前驱体法制备的样品的高温稳定性，我们在 800℃ 和 1000℃ 高温分别对此粉体进行了焙烧。由图 7 的 TEM 照片可见，高分子前驱体法制备的样品经 800℃、1000℃ 高温焙烧 2h 后，颗粒大小仍较均匀，平均颗粒大小在 60nm 和 80nm 左右，基本无团聚烧结现象，这表明采用该方法可有效抑制晶粒增长及高温烧结，这对该材料用于汽车尾气催化剂提供了很有意义的信息。

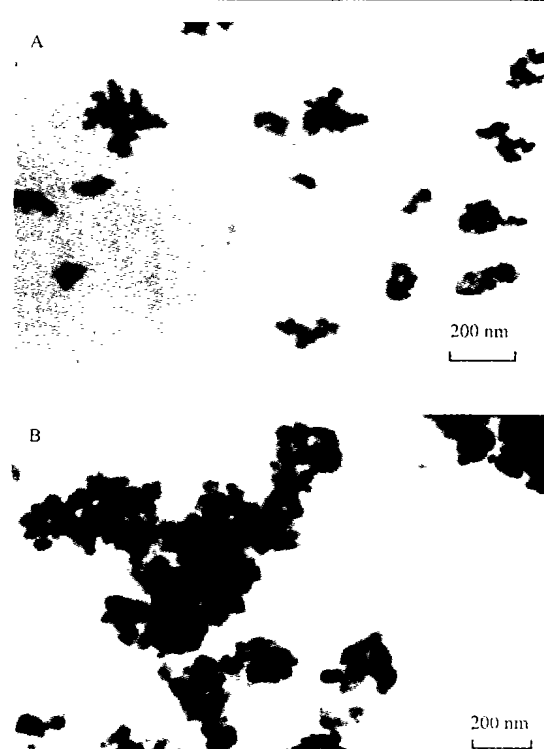


图 7 不同焙烧温度后高分子前驱体法制备样品的 TEM 照片

Fig. 7 TEM micrographs of samples by polymeric precursor method at (A) 800℃, (B) 1000℃

3 结 论

(1) 采用高分子前驱体法和柠檬酸盐凝胶法均可制成纳米级的 Ce-Zr-Ba-O 复合氧化物粉体。高分子前驱体法和柠檬酸盐凝胶法相比，可制得高比表面积 Ce-Zr-Ba-O 复合氧化物，并且获得了较好的 CO 完全氧化活性结果，由该方法制得的 Ce-Zr-Ba-O 复合氧化物粉体的晶相形成温度较低。

(2) 高分子前驱体法制备的样品经 1000℃ 焙烧后，其粒子没有出现明显的团聚及晶粒增长现象，表明其有较好的热稳定性。

参 考 文 献

- [1] Shyu J. Z., Webber W. H., Gandhi H. S. *J. Phys. Chem.*, 1988, 92, 4964.
- [2] HU Yu-Hai(胡玉海), GAO Jian(高健) et al *Gaodeng Xuexiao Huaxue Xuebao(Chem. J. Chinese Universities)*, 2001, 22, 1735.
- [3] XIAO Li(肖莉), LIN Pei-Yan(林培琰) et al *Fenzi*

- Cuihua (*Journal of Molecular Catalysis*), **2000**, **14**(2), 81.
- [4] Christine B., Nolven G., Edouard G., Michel P. *Catalysis Today*, **2000**, **59**, 33.
- [5] Zamar F., Trovarelli A., Leitenburg C. de et al *J. Chem. Soc. Chem. Commun.*, **1995**, 965.
- [6] GUO Yun(郭耘), LI Shu-Ben(李树本) et al *Fenzi Cuihua (Journal of Molecular Catalysis)*, **2000**, **14**(1), 41.
- [7] Jones S. L., Norman C. J. *J. Am. Ceram. Soc.*, **1988**, **71**, 190.
- [8] JIU Jin-Ting(酒金婷), GE Yue(葛 钥) et al *Wuji Cailliao Xuebao (Journal of Inorganic Materials)*, **2001**, **16**(5), 867.
- [9] Fornasiero P., Kašpar J. et al *Journal of Catalysis*, **1997**, **167**, 576.
- [10] WANG En-Guo(王恩过), CHEN Song-Ying(陈诵英) *Zhongguo Xitu Xuebao (Journal of the Chinese Rare Earth Society)*, **2001**, **19**(1), 17.

Synthesis and Catalytic Properties of Nanosized Ce-Zr-Ba-O

ZHANG Pei-Zhuang¹ CHEN Min^{*、1} WANG Yue-Juan² ZHENG Xiao-Ming¹

(¹ Institute of Catalysis, Zhejiang University, Hangzhou 310028)

(² Institute of Physical Chemistry, Zhejiang Normal University, Jinhua 321004)

Ce-Zr-Ba-O mixed oxides were prepared by two different methods, such as polymeric precursor method and citrate gel method. The catalysts were investigated by XRD, TEM, BET surface area and TG-DTA technologies. The results indicated that the nanosized particles were formed in both catalysts. Comparing the two methods, the catalyst prepared by polymeric precursor method showed the remarkable surface area, good thermal stability and high CO oxidation activity, and which was corresponding with the particle size.

Keywords: preparation method nanosized particle Ce-Zr-Ba-O catalyst